New Journal of Physics
The open-access journal for physics

Surface states dominative Au Schottky contact on vertical aligned ZnO nanorod arrays synthesized by low-temperature growth

Ke Cheng[1,2], Gang Cheng[1], Shujie Wang[1], Linsong Li[1], Shuxi Dai[1], Xingtang Zhang[1], Bingsuo Zou[2] and Zuliang Du[1,3]

[1] Key Laboratory for Special Functional Materials, Henan University, Kaifeng, 475001, People's Republic of China
[2] Institute of Physics, Chinese Academy of Sciences, Beijing, 100080, People's Republic of China
E-mail: zld@henu.edu.cn

New Journal of Physics **9** (2007) 214
Received 2 May 2007
Published 6 July 2007
Online at http://www.njp.org/
doi:10.1088/1367-2630/9/7/214

Abstract. Vertical aligned ZnO nanorod (diameter = 50 nm) arrays on indium tin oxide (ITO) substrates have been grown using a new two-step soft chemical procedure. The resulting current–voltage (*I–V*) characteristics of the ZnO nanorods exhibited a clear rectifying behaviour. This rectifying behaviour was attributed to the formation of a Schottky contact between the Au coated atomic force microscopy (AFM) tip and ZnO nanorod (nano-M/SC) which was dominated by the surface states in ZnO itself. Photo-assisted conductive AFM (PC-AFM) was used to demonstrate how the *I–V* characteristics are influenced by the surface states. Our *I–V* results also showed that the nano-M/SCs had a good photo-electric switching effect at reverse bias.

[3] Author to whom any correspondence should be addressed.

Contents

1. Introduction

Due to its low-cost, large band-gap, and luminescent properties, ZnO has become an important environmentally friendly wide band-gap semiconductor material. It has been widely investigated in many fields and has begun to show some potential applications in gas sensors, piezoelectric devices, electroacoustic transducers, and solar cells [1]. For the potential applications of ZnO in nano-electronic and nano-optoelectronic devices, substantial efforts have been devoted to develop novel synthetic methodologies of one-dimensional (1D) ZnO nanostructures [2]. The well-established methods include metalorganic chemical-vapour deposition (MOCVD), vapour liquid solid epitaxial (VLSE), pulsed laser deposition (PLD), and templating using anodic alumina membranes [3, 4]. However, all the above methods require expensive equipment and need to be done under extreme conditions such as high temperature, high pressure. Therefore, a low-temperature, large-scale, and versatile synthetic process is preferred. At the same time, understanding 1D ZnO's transport properties and its interactions with metal contacts (metal/semiconductor, i.e. M/SC) are also important issues before it is fabricated into real electronic devices. Recently, the electrical properties of ZnO contacting with different metals have been extensively studied [5]–[8]. Two kinds of distinct current–voltage (*I–V*) characteristics have been observed depending on the Fermi surface alignment between the metals and ZnO. One is almost linear due to the formation of an Ohmic contact; another is almost rectifying due to the formation of a Schottky contact. In general, high reactivity metals (such as Al, Pt/Ga, Ti/Au, Ta/Au, Al/Pt, and Ti/Al) can form Ohmic contacts with *n*-ZnO [9–13], while low reactivity metals (such as Au, Ag, and Pd) can form Schottky contacts with *n*-ZnO [14–19]. However, the rectifying behaviour has been only observed for 1D ZnO. And the ideality factors of such ZnO Schottky contacts are considerably higher than unity [5, 6, 8]. The large deviation of the ideality factor has been simply proposed by the impacts of asymmetric contact, or the influence of interfacial layers and surface states [5–8]. In fact, the *I–V* characteristics of nanomaterials' contacts with different metals (nano-M/SCs) should be mostly dominated by the surface states because there are usually abundant surface states existing on the surface of nanomaterials [20]. However, only a few reports have been found to illustrate how the surface states influence the rectifying behaviour of the nano-M/SCs [6].

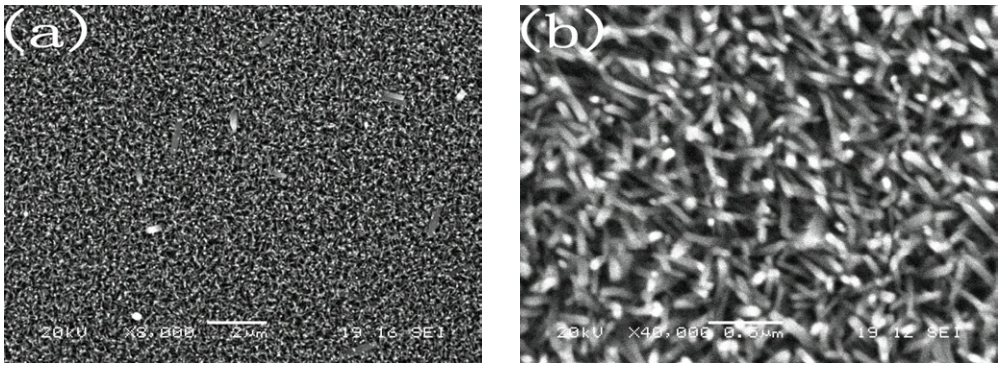

Figure 1. Typical SEM top-view images of the as prepared ZnO nanorod films on the ITO substrate at (a) low and (b) high magnifications, respectively.

Here, we adopted a two-step chemical process to produce vertical aligned ZnO nanorods on the ITO substrate, and investigated the *I–V* properties between an atomic force microscopy (AFM) tip and ZnO nanorods. Through our photo-assisted conductive AFM (PC-AFM) measurements, the influences of surface states on the rectifying behaviour of the Schottky contact were illustrated. At the same time, the response for UV illumination of the nano-M/SCs was also investigated.

2. Experimental

The typical procedure for the ZnO nanorod array synthesis was as follows: firstly, 4 nm diameter ZnO nanoparticles were prepared from zinc acetate dehydrate in alcoholic solution, which was a modified method developed by Henglein *et al* [20]. Then, ZnO nanoparticles were directly deposited onto the indium tin oxide (ITO) substrate using the Langmuir–Blodgett (LB) method to form a 50–200 nm thick ZnO nanoparticle film as crystal seeds. This film was heated in air at 300 °C for 5 h before growing nanorods. Secondly, the as-prepared crystal seeds film on ITO substrate was suspended upside-down in an aqueous solution including zinc nitrate hydrate (0.025 M) and methenamine (0.025 M) at 90° C for 1.5 h. Finally, the substrate was removed from the solution, thoroughly washed with deionized water, and dried by N_2 at room temperature.

3. Results and discussion

3.1. Characterization of the prepared ZnO nanorod arrays

As shown in figure 1, the whole ITO substrate was coated with highly uniform and densely packed ZnO nanorods. Although the nanorods were not perfectly aligned on the substrate, they showed a tendency to grow perpendicular to the surface. The average diameter of ZnO nanorods was about 40–50 nm with a narrow wire–wire distance.

X-ray diffraction (XRD) patterns were measured by a X'Pert Pro x-ray diffractometer using Cu K-alpha radiation. As shown in figure 2, Only the remarkably enhanced [002] reflection peak with a hexagonal crystal structure was observed. This indicated that ZnO nanorods were grown with c-axis orientation and almost perpendicular to the substrate surface as observed in the scanning electron microscope (SEM) images.

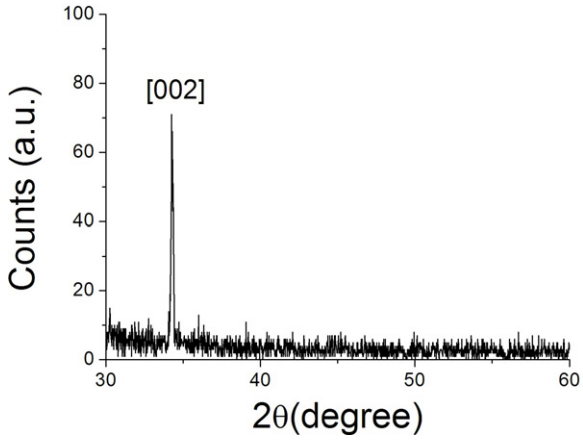

Figure 2. The XRD pattern of the prepared ZnO nanorod array on the ITO substrate.

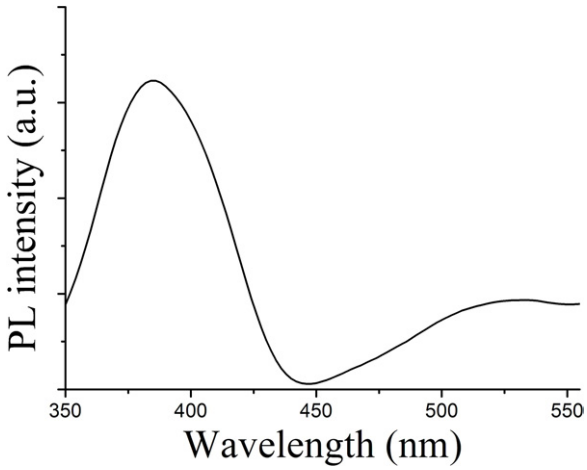

Figure 3. PL of ZnO nanorods film.

A typical room-temperature photoluminescence (PL) spectrum of the as prepared ZnO nanorod arrays was shown in figure 3. A UV emission band was found at around 380 nm, which can be assigned to the well-known recombination of excitons. A broad and weak green emission was observed centering at 535 nm, which was related to the PL of surface states [21]. This indicated that the nanorods obtained in our experiment had abundant surface states on the surface.

3.2. Schematic diagram of our measurement set-up and dynamic force microscopy (DFM) images of ZnO nanorod array

Conductive AFM (C-AFM) and PC-AFM are employed to investigate the electrical properties of the system. Generally, C-AFM has been one of the most successful tools for both morphology and electronic property measurements [5, 22, 23]. The conductive AFM probe is able to touch a nm-scale spot on the sample in which a bias voltage can be applied directly onto its surface, enabling us to investigate the electric properties of the sample. Meanwhile PC-AFM can allow us to study the photo-generated carriers transport properties on the nanoscale. In our *I–V* set-up, we adopted

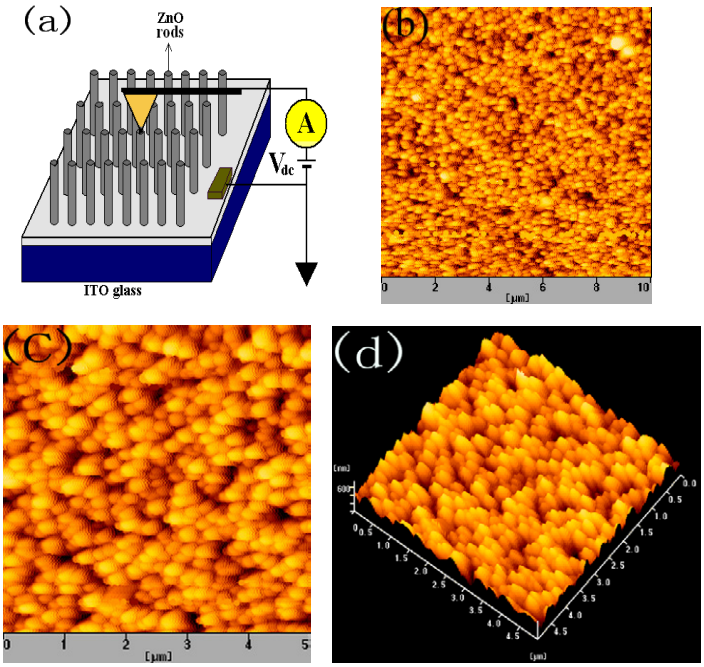

Figure 4. (a) Schematic diagram of the PC-AFM measurement; (b) large scale DFM image of ZnO nanorods on the ITO substrate; (c) and (d) small scale DFM image of ZnO nanorods on the ITO substrate and the corresponding 3D image.

a tip/sample layout as shown in figure 4(a). Obviously, a metal/semiconductor point contact was formed by placing an Au-coated conducting tip on the top surface of an individual ZnO nanorod. *I–V* characteristics with and without UV light irradiation were measured by applying a low voltage to the conductive AFM tip positioned directly on top of the ZnO nanorod. All measurements were performed at room temperature. Every *I–V* characteristic curve was plotted by measuring 15 times and averaging the data.

Prior to the electrical characteristic measurements, the morphologies of ZnO nanorod arrays were obtained using a tapping mode AFM (DFM). As shown in figures 4(b)–(d), the DFM images of ZnO nanorod arrays exhibited a larger diameter than that observed in SEM images. This distortion resulted from the tip convolution effect due to the high aspect ratio of the nanorod [5].

3.3. I–V characteristics of Au coated AFM tip and ZnO nanorod contact

In our PC-AFM measurements, the *I–V* characteristics were obtained at a contact force of 20 nN in the dark and under UV ($\lambda = 350$ nm) illumination. The applied bias voltage ranged from -7 V to $+7$ V. The point contact on the ZnO nanorod exhibited a clear nonlinear and asymmetric behaviour in their *I–V* curves as shown in figure 5(a). The *I–V* curve in the dark showed a turn-on voltage of 1.2 V for the forward bias and a breakdown voltage of -4.8 V for the reverse bias. It was a typical soft breakdown at this voltage as evidenced by the low-leakage-current behaviour after biasing down to the breakdown voltage [19]. In our experiment, we adopted an asymmetric Au/ZnO nanorods/ZnO seed film/ITO contact, instead of a symmetric Au/ZnO/Au structure used in the literature [6, 8]. The contact between ZnO nanorods/ZnO seed film/ITO junction

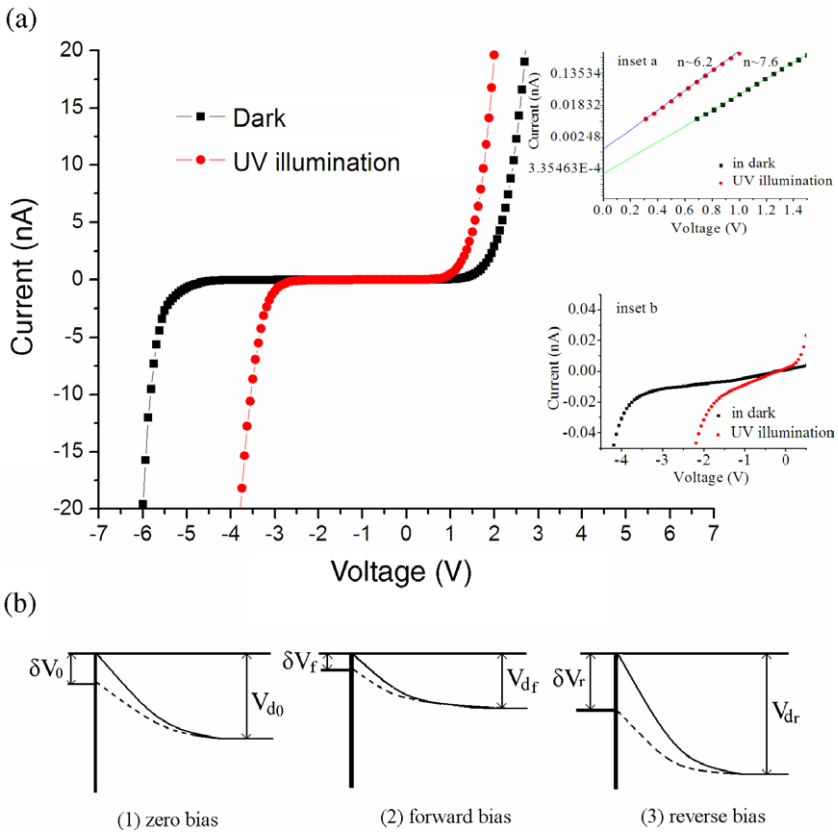

Figure 5. (a) *I–V* curves of ZnO nanorod in the dark (black) and under UV illumination conditions (red). (b) Schematic diagram of Schottky potential barrier changes under different bias and illumination. The inset a is ln(*I*) versus *V* curve in the dark and under illumination; inset b is the magnification of figure 5(a).

was a barrier-free Ohmic contact due to the lower work function of ITO itself [5]. Therefore, we concluded that the nonlinear and rectifying behaviour of the *I–V* characteristic resulted from the single Schottky contact between the AFM tip and ZnO nanorod.

For thermoionic emission theory and V greater than $3KT/q$, the general diode equation in forward bias is [18, 19]

$$I = I_s \exp\left[\frac{q\,(V - IR_s)}{nK_BT}\right], \tag{1}$$

where I is the current, I_s is the reverse bias saturation current, K_B is the Boltzmann's constant, T is the absolute temperature ($T = 300$ K), q is the unit charge of an electron, R_s is the series resistance, V is the applied voltage and n is the ideality factor. The ideality factor was determined to be ~7.6 in terms of the theoretical fitting of equation (1) and was shown in figure 5(a) (insert a, in the dark). It was much larger than one, which suggested that the AFM tip/ZnO nanorod Schottky diode was different from conventional Schottky diode behaviour. The higher value of n was probably due to the existence of interfacial layers or surface states [5]–[8], [15].

Since ZnO readily forms an interfacial layer (mainly including adsorbed oxygen, hydroxide, moisture, etc) on the surface which always had a thickness of one or two monolayers [15, 16]. These would result in the existence of abundant surface states on the ZnO surface. And this was

also confirmed from our PL result in figure 3. Here, we noticed that the interfacial layer thickness at one or two monolayers may affect the chemical properties of materials deeply. But for the *I–V* measurement, we can neglect the influence of interfacial layers as the electrons could easily pass through by the tunnelling effect [15]. So the higher value of n must due to the existence of surface states. The high density of surface states would generate an upward band bending and then form a potential barrier on the surface, which was almost independent of the work function of the metal due to the so-called pinning of Fermi energy. That is, the barrier height did not follow the difference in the work function value, but was mostly dominated by the surface states or band bending in ZnO itself as pointed out by Bardeen [24] and others [25, 26]. When the density of surface states was high enough, the barrier height controlled by the surface states must dominate the *I–V* rectifying behaviour [26, 27]. And the rectifying behaviour observed in our experiment was just this case as shown in figure 5(a).

To further investigate the influence of the surface states (i.e. the surface band bending) on rectifying behaviour, we studied the different photoresponse under forward and reverse biases. Clearly, different threshold voltages under reverse and forward biases were observed in our photo-assisted *I–V* measurement (figure 5(a) red line). The turn-on voltage was dropped from 1.2 to 0.8 V for the forward bias and the breakdown voltage was dropped from −4.8 to −2.8 V for the reverse bias under the UV illumination. The lower turn-on voltage implied the Schottky barrier height decreased. In fact, the Schottky barrier height, Φ_{SB}, could be estimated from the reverse saturation current I_s, which is given by $I_s = A^* A T^2 \exp(-\Phi_{SB}/kT)$, where A^* is the Richardson constant, A is the contact area [18, 19]. I_s could be obtained from the curve of ln(I) versus V. The curve of ln(I) versus V under UV illumination (0.3–0.6 V) is shown in figure 5(a) (insert a, under UV illumination). From the fitting curves, we found that the Schottky barrier height decreased about 40 mV under UV illumination.

The surface band bending change under illumination has been widely investigated using the well-established contactless surface photovoltage (SPV) method, i.e. SPV spectroscopy (SPS) which relies on analysing illumination-induced changes in the surface voltage [28]–[31]. For the n-type semiconductor character of ZnO, an upward band bending was formed on the surface of ZnO due to the existence of surface states. Then a built-in field could be formed with a direction from the bulk toward the surface. When a forward bias was applied, whose direction was reverse to the built-in field, the surface band bending was decreased. Contrarily, when a reverse bias was applied, the surface band bending increased upward because the direction was coincident with the built-in field [25, 27, 31] (as shown in figure 5(b) solid lines). The different surface band bending indicated the intensity of the built-in field was different, and then affected the separation efficiency of excitons [32]. When the UV light was imposed on ZnO nanorods, photo-generated excitons were separated by the built-in field. Under forward bias, the separation efficiency of photogeneration carriers (i.e. excitons) reduced due to the weakened built-in field. And then a smaller surface band bending change δV_f was obtained. While a larger surface band bending change δV_r was obtained under reverse bias for the increased carrier separation efficiency (as shown in figure 5(b) dashed lines). Therefore a different threshold voltage change was observed in our PC-AFM measurement due to the different band bending change under reverse and forward bias as discussed above.

On the other hand, the presence of surface states would also result in the directional move of photogenerated carriers, thereby increasing the current both for forward and reverse biases when illuminated. Especially for reverse biases, the current would increase more due to the existence of stronger field in the surface of semiconductor [26, 27]. Actually, we obtained the

ideality factor 6.2 under UV illumination (from the insert a of figure 5(a), which was smaller than that of 7.6 in the dark. This indicated the current was increased somewhat. The reverse leakage current was increased obviously under UV illumination (see insert b of figure 5(a), which caused the breakdown voltage to be down extremely [33, 34]. So we believed that the large decrease of the breakdown voltage under UV illumination mainly resulted from the increase of reverse leakage current. And we found the large change of the reverse breakdown voltage enabled the nano-M/SCs to have good photo-electronic switching effect. For example, the current ratio of tune-on/off was up to 10^3 at -3.8 V.

From the above discussion, we believed that the contact properties between ZnO nanorod and different metals were mainly dominated by surface states rather than the work function value of the metals and other factors. Therefore, we can easily understand why the contacts were Ohmic contacts with a linear *I–V* behaviour or Schottky contacts with a rectifying *I–V* behaviour. That is, for ZnO crystal, the contacts might be Ohmic if the surface states were cleared completely (see references [9]–[13], in which the metal-doped method was generally used); otherwise, the contacts would be Schottky [14]–[19]. In fact, the SPS study of ZnO nanoparticles and nanorods had also indicated that the SPV signal would disappear if the surface states were cleaned [35, 36]. For nano-M/SCs, they were usually Schottky contacts owing to the existence of abundant surface states on the nanomaterials surface [5]–[8]. Also we can easily understand why the Schottky diodes ideality factor n reported in the literature always had so large a deviation.

4. Conclusions

In summary, we adopted a simple two-step seeding process to produce vertical aligned ZnO nanorod arrays on an ITO substrate. The PL spectra showed that the nanorods had abundant surface states. The *I–V* characteristics of the vertical aligned ZnO nanorod arrays were investigated by C-AFM and showed clear nonlinear and asymmetrical rectifying behaviour. Our PC-AFM measurement was used to determine the influence of the surface states on the *I–V* characteristics. The results indicated that UV illumination could cause a decrease of barrier height and an increase of reverse current, which resulted in the decrease both of forward turn-on and reverse breakdown voltage. And a good photo-electronic switching effect was also observed in our PC-AFM measurement.

Acknowledgments

This work was supported by Natural Science Foundation of China (no. 90306010, 20371015 and 20173073), Program for New Century Excellent Talents in University of China (NCET-04-0653) and Nanodevice key project of CAS. The authors express their appreciation to Prof. Zhonglin Wang and Professors Dejun Wang for helpful discussions.

References

[1] Feng X J, Feng L, Jin M H, Zhai J, Jiang L and Zhu D B 2004 *J. Am. Chem. Soc.* **126** 62

[2] Heo Y W, Norton D P, Tien L C , Kwon Y, Kang B S, Ren F, Pearton S J and LaRoche J R 2004 *Mater. Sci. Eng.* R **47** 1

[3] Zheng M J, Zhang L D, Li G H and Shen W Z 2002 *Chem. Phys. Lett.* **363** 123

[4] Haung M H, Wu Y Y, Feick H, Tran N, Webber E and Yang P D 2001 *Adv. Mater.* **13** 113
[5] Park W I, Yi G C, Kim J W and Park S M 2003 *Appl. Phys. Lett.* **82** 4358
[6] Harnack O, Pacholski C, Weller H, Yasuda A and Wessels J M 2003 *Nano Lett.* **3** 1097
[7] Zhang Z Y, Jin C H, Liang X L, Chen Q and Peng L M 2006 *Appl. Phys. Lett.* **88** 073102
[8] Lao C S, Liu J, Gao P X, Zhang L Y, Davidovic D, Tummala R and Wang Z L 2006 *Nano Lett.* **2** 263
[9] Kim H K, Han S H, Seong T Y and Choi W K 2000 *Appl. Phys. Lett.* **77** 1647
[10] Lee J M, Kim K K, Park S J and Choi W K 2001 *Appl. Phys. Lett.* **78** 3842
[11] Kim H K, Kim K K, Park S J, Adesida I and Seong T Y 2003 *J. Appl. Phys.* **94** 4225
[12] Inumpudi A, Iliadis A A, Krishnamoorthy S, Choopun S, Vispute R D and Venkatesan T 2005 *Solid-State Electron.* **46** 1665
[13] Iliadis A A, Vispute R D, Venkatesan T and Jones K A 2002 *Thin Solid Films* **420–1** 478
[14] Auret F D, Goodman S A, Legodi M J, Look D C and Meyer W E 2002 *Appl. Phys. Lett.* **80** 1340
[15] Coppa B J, Davis R F and Nemanich R J 2003 *Appl. Phys. Lett.* **82** 400
[16] Coppa B J, Fulton C C, Hartlieb P J, Rodriguez B J, Shields B J, Nemanich and Davis R F 2004 *J. Appl. Phys.* **95** 5856
[17] Polyakov A Y, Smirnov N B, Kozhukhova E A , Vdovin V I, Ip K, Heo Y W, Norton D P and Pearton S J 2003 *Appl. Phys. Lett.* **83** 1575
[18] Ip K, Heo Y W, Baik K H, Norton D P, Kim S, LaRoche J R, Ren F and Pearton S J 2004 *Appl. Phys. Lett.* **84** 2835
[19] Oh D C, Kim J J, Makino H, Hanada T, Cho M W, Ko H J and Yao T 2005 *Appl. Phys. Lett.* **86** 042110
[20] Haase M, Weller H and Henglein A 1988 *J. Phys. Chem.* **92** 482
[21] Yao B D, Chan Y F and Wang N 2002 *Appl. Phys. Lett.* **81** 757
[22] Wang S J, Zhang X T, Cheng G, Jiang X H, Li Y C, Huang Y B and Du Z L 2005 *Chem. Phys. Lett.* **405** 63
[23] Wang S J, Cheng G, Jiang X H, Li Y C, Huang Y B and Du Z L 2006 *Appl. Phys. Lett.* **88** 212108
[24] Bardeen J 1947 *Phys. Rev.* **71** 717
[25] Morrison S R 1977 *The Chemical Physics of Surface* (New York: Plenum)
[26] Rhoderick E H 1978 *Metal-Semiconductor Contacts* (Oxford: Clarendon)
[27] Mönch W 1990 *Rep. Prog. Phys.* **53** 221
[28] Johnson E O 1958 *Phys. Rev.* **111** 153
[29] Heiland G. and Mönch W. 1973 *Surf. Sci.* **37** 30
[30] Luth H 1975 *Appl. Phys.* **8** 1
[31] Kronik L and Shapira Y 1999 *Surf. Sci. Rep.* **37** 1
[32] Xie T F, Wang D J, Zhu L J, Wang C, Zhou X Q, Wang M and Li T J 2000 *J. Phys. Chem.* B **104** 8177
[33] Tyagi M S 1968 *Solid-State Electron.* **11** 117
[34] Motayed A, Davydov A V, Vaudin M D, Levin I, Melngailis J and Mohammad S N 2006 *J. Appl. Phys.* **100** 024306
[35] Lin Y H, Wang D J, Zhao Q D, Yang M and Zhang Q L 2004 *J. Phys. Chem.* B **108** 3202
[36] Lin Y H, Wang D J, Zhao Q D, Li Z H, Ma Y D and Yang M 2006 *Nanotechnology* **17** 2110